

# Pathogen-Driven Outbreaks in Forest Defoliators Revisited: Building Models from Experimental Data

Greg Dwyer,<sup>1,\*</sup> Jonathan Dushoff,<sup>2</sup> Joseph S. Elkinton,<sup>3</sup> and Simon A. Levin<sup>4</sup>

1. Department of Biological Science, University of Notre Dame, Notre Dame, Indiana 46556;

2. Institute of Physics, Academia Sinica, Nankang 11529 Taipei, Taiwan;

3. Department of Entomology, University of Massachusetts, Amherst, Massachusetts 01003-2410;

4. Department of Ecology and Evolution, Princeton University, Princeton, New Jersey 08544

Submitted July 12, 1999; Accepted March 7, 2000

---

**ABSTRACT:** Models of outbreaks in forest-defoliating insects are typically built from a priori considerations and tested only with long time series of abundances. We instead present a model built from experimental data on the gypsy moth and its nuclear polyhedrosis virus, which has been extensively tested with epidemic data. These data have identified key details of the gypsy moth–virus interaction that are missing from earlier models, including seasonality in host reproduction, delays between host infection and death, and heterogeneity among hosts in their susceptibility to the virus. Allowing for these details produces models in which annual epidemics are followed by bouts of reproduction among surviving hosts and leads to quite different conclusions than earlier models. First, these models suggest that pathogen-driven outbreaks in forest defoliators occur partly because newly hatched insect larvae have higher average susceptibility than do older larvae. Second, the models show that a combination of seasonality and delays between infection and death can lead to unstable cycles in the absence of a stabilizing mechanism; these cycles, however, are stabilized by the levels of heterogeneity in susceptibility that we have observed in our experimental data. Moreover, our experimental estimates of virus transmission rates and levels of heterogeneity in susceptibility in gypsy moth populations give model dynamics that closely approximate the dynamics of real gypsy moth populations. Although we built our models from data for gypsy moth, our models are, nevertheless, quite general. Our conclusions are therefore likely to be true, not just for other defoliator–pathogen interactions, but for many host–pathogen interactions in which seasonality plays an important role. Our models thus give qualitative

insight into the dynamics of host–pathogen interactions, while providing a quantitative interpretation of our gypsy moth–virus data.

*Keywords:* host–pathogen interactions, mathematical models, *Lymantria dispar*, nuclear polyhedrosis virus, heterogeneity in susceptibility.

---

A classic ecological argument is that the occurrence of cycles in predator–prey models suggests that fluctuations in animal populations may be driven by biotic interactions rather than by weather (Elton 1927). More recent versions of this argument use more sophisticated statistical methods (Turchin 1990; Turchin and Taylor 1992; Ellner and Turchin 1995) and so make the argument in favor of biotic interactions with greater force. We are likewise interested in fluctuations in animal populations, specifically in outbreaks of forest insects, but we assume that outbreaks in at least some insects are driven by biotic interactions. We focus instead on mechanism. We ask, How likely is it that pathogens are the mechanism driving insect outbreaks? This idea originated in modeling papers by Anderson and May (1980, 1981), but Anderson and May's models have been criticized on the grounds that they make unrealistic assumptions. Modifications to their models, however, have not been particularly enlightening because some modifications make it more likely that the models will show the long-period cycles typical of defoliating insects, while other modifications make such cycles less likely (see Briggs et al. 1995 for a review).

We argue that part of the difficulty in determining the importance of pathogens in insect outbreaks is that previous models have been constructed from a priori considerations and have been tested only by comparison with time series data on insect abundances. Here, we present an alternative approach that is focused on a particular insect–pathogen interaction, between the gypsy moth *Lymantria dispar* and its nuclear polyhedrosis virus, and that is based on experimental data. In previous work, we used field experiments to show that the transmission of the gypsy moth virus is determined largely by host and pathogen density and by host heterogeneity in susceptibility (Dwyer and Elkinton 1993; D'Amico and Elkinton 1995;

\* Present address: Department of Ecology and Evolution, University of Chicago, Chicago, Illinois 60637; e-mail: gdwyer@midway.uchicago.edu.

D'Amico et al. 1996, 1998; Dwyer et al. 1997). We further showed that an epidemic model that includes these factors can predict the timing and intensity of single-season epidemics in real gypsy moth populations (Dwyer et al. 1997, 2000) in the gypsy moth, and in many other temperate-zone defoliators, there can be only one virus epidemic and one host generation per year). Other experiments have shown that the overwinter survival of the virus on egg masses largely determines the density of virus at the beginning of the epidemic (Murray and Elkinton 1989, 1990). Here, we consider what these experimental data imply for gypsy moth population dynamics by combining our epidemic model with a model for overwinter virus survival. The resulting model differs from the Anderson and May model and most of its successors (but see Briggs and Godfray 1996) by allowing for heterogeneity in susceptibility among hosts, by including the details of virus survival, and by allowing for delays between infection and death.

Although we focus on the gypsy moth and its virus, the similarity between the gypsy moth virus and pathogens of other defoliators suggests that our model will be applicable to many other pathogens of forest defoliators (Cory et al. 1997). We therefore ask two related questions. First, we ask, How does host heterogeneity in transmission and developmental delays affect the likelihood of long-period, large-amplitude fluctuations in host-pathogen interactions? Second, we focus more specifically on the gypsy moth, and we ask, How does heterogeneity in host susceptibility affect gypsy moth population dynamics? In particular, our gypsy moth data show moderately high levels of heterogeneity in host susceptibility. Such heterogeneity generally has a strongly stabilizing effect on interspecific interactions (Hassell et al. 1991), yet gypsy moths in North America, where the virus is of great importance (Elkinton and Liebhold 1990), are known to have unstable population dynamics (Williams and Liebhold 1995). We therefore ask, Are the levels of heterogeneity in susceptibility estimated from our data consistent with the outbreaking dynamics of the gypsy moth in North America?

### Modeling Single Epidemics

For host-pathogen interactions with only one epidemic per year, we can model the epidemic and interepidemic periods separately. First, we describe our epidemic model. This model was built from experiments on the transmission of the gypsy moth virus, but the underlying biology is common to the pathogens of many defoliators (Evans and Entwistle 1987; Cory et al. 1997). These viruses are transmitted horizontally when host insects, while feeding,

accidentally consume contaminated foliage. Larvae that consume a high enough dose (only larvae can become infected; Volkmann 1997) die in about 2 wk, and their cadavers further contaminate the foliage. If the virus particles in these cadavers are not killed by the ultraviolet rays in sunlight or otherwise removed from the foliage, the virus is available to be consumed by other insects, leading to new rounds of transmission. We have shown experimentally that per capita transmission is unaffected by prior defoliation (D'Amico et al. 1998) and is only slightly influenced by moisture (D'Amico and Elkinton 1995). Our experiments have shown, however, that per capita transmission is strongly affected by virus density and by heterogeneity among individuals in the dose required to cause infection (Dwyer and Elkinton 1993; Dwyer et al. 1997). A model that allows for these effects is

$$\frac{\partial S}{\partial t} = -\nu PS, \quad (1)$$

$$\frac{dP}{dt} = P(t - \tau) \int_0^\infty \nu S(\nu, t - \tau) d\nu - \mu P \quad (2)$$

where  $S$  is the density of uninfected insects,  $P$  is the density of infectious cadavers,  $\nu$  determines the rate of horizontal transmission of the disease,  $\tau$  is the time between infection and death, or the pathogen generation time, and  $\mu$  is the breakdown rate of the cadavers on the foliage. Note that we do not need to include an equation for infected hosts  $I$  because all infected hosts are ultimately converted to cadavers so that new cadavers at time  $t$  can be calculated from the number of hosts infected  $\tau$  time units earlier. We are thus assuming that there is a constant time lag  $\tau$  between infection and death, which is important because the time that it takes an infected insect to die is a significant fraction of the length of an epidemic. The resulting model is very similar to models originally constructed to describe the dynamics of human diseases (Kermack and McKendrick 1927). An important difference from classical disease models, however, is that equations (1) and (2) allow for variability among individuals in susceptibility and so resemble AIDS models that allow for variability in levels of sexual activity (Anderson et al. 1986). This variability in host susceptibility is reflected in a distribution of transmission parameters  $\nu$  so that  $S(\nu, t)d\nu$  gives the number of larvae at time  $t$  that have susceptibilities between  $\nu$  and  $\nu + d\nu$  for small  $d\nu$ . In particular, we assume that  $S(\nu, 0) = \hat{S}(0)f(\nu)$ , where  $\hat{S}(0)$  is the density of hosts at the beginning of the epidemic ( $\hat{S}(0) \equiv \int_0^\infty S(\nu, 0)d\nu$ ) and  $f(\nu)$  is the initial distribution of transmission rates. In much of what follows, we assume that  $f(\nu)$  is a gamma distribution, which is mathematically convenient and

which matches our data (Dwyer et al. 1997). Our results, however, can also be derived without this assumption, by using an approximation method (app. A).

One of the advantages of our model structure is that it allows us to understand the long-term dynamics of host-pathogen interactions in terms of single epidemics. To make this connection, we first show how single epidemics, as described by equations (1) and (2), are affected by host and pathogen density, host heterogeneity in susceptibility, and epidemic length. A convenient way to see these effects is to allow time to go to infinity in equations (1) and (2). We call this approximation the “infinite epidemic” or “burnout” approximation, and it corresponds to allowing the epidemic to burn itself out rather than be truncated by host pupation, as sometimes occurs in gypsy moth populations. When initial host and pathogen densities are large or when the length of the season is long compared to the pathogen generation time, the approximation is quite accurate. It provides an implicit expression for the fraction of hosts infected, according to

$$1 - I = \left[ 1 + \frac{\bar{\nu}C^2}{\mu} \left[ \hat{S}(0) + P(0) \right] \right]^{-1/C^2}. \quad (3)$$

Here,  $I$  is the fraction of the host population that becomes infected in the epidemic,  $\hat{S}(0)$  is again the total initial host density,  $P(0)$  is the initial pathogen density, and  $\bar{\nu}$  and  $C$  are the mean and coefficient of variation of the distribution of host susceptibility (app. A). To interpret equation (3), we express both pathogen and host density in terms of the threshold density  $N_T = \mu/\bar{\nu}$ , which is the host density necessary for an epidemic to occur as the initial pathogen density  $P(0)$  approaches 0. The fraction infected  $I$  thus depends only on the heterogeneity  $C$  and the rescaled densities  $\hat{S}(0)/N_T$  and  $P(0)/N_T$ . For this scaling, figure 1 shows that higher densities of hosts or pathogens lead to more intense epidemics, as we would expect. Note that increases in the transmission rate or decreases in the breakdown rate have the same effect on the fraction infected  $I$  as do proportional increases in the initial densities of hosts and pathogens. Figure 1 additionally shows that increasing heterogeneity in susceptibility leads to smaller epidemics, even with mean susceptibility held constant, implying that the addition of more resistant individuals has a greater effect on epidemic intensity than does the addition of more susceptible individuals. Changes in heterogeneity, however, do not affect the threshold density.

Because only larvae can become infected, and because the time between infection and death  $\tau$  is often a significant fraction of the larval period, epidemics in real insect populations may often be curtailed by host pupation. Figure 1 compares the fraction infected for a model that allows

for epidemics that are shortened by pupation, calculated from equations (1) and (2), to the fraction infected as calculated by the infinite-epidemic approximation (3). Surprisingly, the approximation works well even if the epidemic lasts for only five times the pathogen-generation time  $\tau$ . In gypsy moth, the larval season lasts about 10 wk, and the pathogen generation time  $\tau$  is about 10–14 d (Woods and Elkinton 1987), for an epidemic length of  $5-7\tau$ . The burnout approximation may therefore work well in many cases. Also, early burnout is more likely when host and pathogen densities are high, so equation (3) becomes a better approximation as densities increase.

### Modeling Long-Term Dynamics

Here, we link together single epidemics, as modeled by either equation (3) or equations (1) and (2), by modeling the reproduction of the surviving hosts and the over-winter survival of the pathogen. In the interests of clarity, we follow previous modeling efforts in assuming that host reproduction is density independent so that the pathogen is the only source of density dependence. Although the fecundity of gypsy moths and other defoliators can be reduced as a result of competition for food at high densities (Campbell 1978; Carter et al. 1991; Myers and Kuken 1995), and survival at low densities may be density dependent (Elkinton et al. 1996), we are partly exploring whether we need to invoke such density dependence to explain the dynamics of these insects, so for now it makes sense to neglect these details. We therefore assume that each host that survives the epidemic produces some constant number of eggs that hatch to start the next year's epidemic.

Like our epidemic model, our model for pathogen survival is based on experimental evidence. Specifically, Murray and Elkinton (1989, 1990) showed experimentally that virus produced during an epidemic contaminates the eggs that are laid afterward. This is significant because virus mortality among hatching larvae is apparently mostly due to infection during emergence from the egg mass (Woods et al. 1991), and these infected hatchlings in turn can initiate another epidemic. The virus can also survive in leaf litter, in pupal mats, and in cracks in bark (Podgwaite et al. 1979), and newly hatched larvae can become infected by walking on these contaminated substrates and transferring the virus to their food plant (Weseloh and Andreadis 1986; Woods et al. 1989). Unlike some fungal pathogens of insects, nuclear polyhedrosis viruses are unable to penetrate the integument of their hosts (see Volkmann 1997). After larvae reach the foliage, however, they generally stay there, except for fifth and sixth instars and some

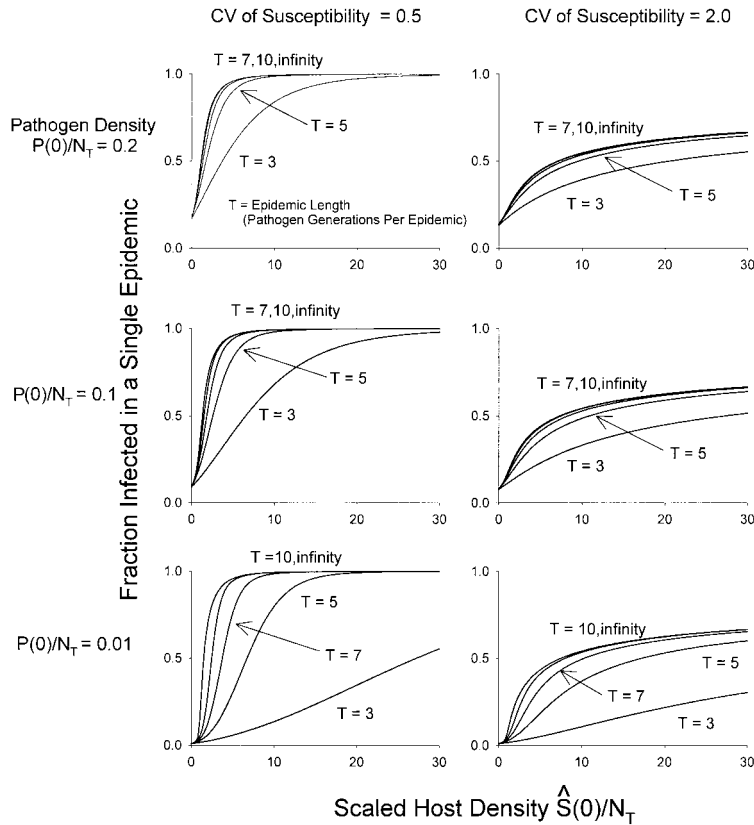


**Figure 1:** Effects of epidemic length  $T$ , number of pathogen generations per epidemic, and coefficient of variation in host heterogeneity in susceptibility  $C$  on epidemic intensity, fraction infected  $I$ . The intensity of infinite epidemics is calculated from the infinite-epidemic equation (3), while the intensity of short epidemics is calculated from the model equations (1)–(2). Note first that the minimum host density at which an epidemic occurs is unaffected by host heterogeneity in susceptibility. Second, the infinite epidemic equation (3) provides a good approximation to equations (1)–(2) for epidemic lengths  $T \geq 5$ .

fourths in low-density populations (Lance et al. 1987; gypsy moths have five larval instars in males and six in females). It therefore appears that infection of larvae as they emerge from the egg is the major process by which the gypsy moth virus overwinters, so in our models, we assume that some fraction  $f$  of the virus produced during the epidemic survives to infect emerging larvae in the following season. A more complex model in which overwintering pathogens can also infect larvae later in the season gave very similar results.

Our model of the infection of hatching larvae is based on our model for the epidemic in later instar larvae, but we allow for a difference in a key parameter. Specifically, for many insects, disease susceptibility is much higher in earlier instars (Watanabe 1987), and for gypsy moth in particular, newly hatched larvae are at least 100 times as susceptible as newly eclosed fourth instars (G. Dwyer, un-

published data). In fact, average susceptibility decreases with each additional larval stage, not just from the first to the second as we have assumed here. The effects of later increases, however, are largely offset by increases in the amount of foliage consumed and by other aspects of feeding behavior (Dwyer 1991; G. Dwyer, unpublished data). Our model for the infection of hatching larvae, which provides the initial conditions for the epidemic, is then

$$S(0, \nu) = N_t f(\nu) e^{-\nu \rho Z_t}, \quad (4)$$

$$P(0) = N_t \int_0^\infty f(\nu) (1 - e^{-\nu \rho Z_t}) d\nu. \quad (5)$$

Here,  $\rho$  is the ratio of the effectiveness of infection at the time of hatch relative to infection later in the season, which

incorporates effects that result from mode of infection, increased susceptibility of larvae, and differences in time of exposure (app. A). Also, to emphasize the differences between our within-season and between-season models, we introduce the new variables  $N_t$  and  $Z_\rho$  which are the initial densities of hosts and pathogens at the beginning of the epidemic in generation  $t$ .

This model assumes that latent infection, an overwintering mechanism whereby virus is transmitted from exposed-but-surviving females to their offspring, is largely unimportant. Although there is some evidence for such infections in other insects (Fuxa and Richter 1992; Rothman and Myers 1994), Murray et al. (1991) showed that the survival of exposed female gypsy moth larvae is low, and no viral DNA can be found in any females that do survive exposure. Moreover, we have established many experimental gypsy moth populations in the field from eggs that have been surface disinfected to rid them of the virus, and such populations have had no virus infections (Gould et al. 1990; Dwyer and Elkinton 1995; Hunter and Elkinton 1999, 2000). We therefore leave latent infections out of our models.

Having linked the epidemic and interepidemic periods, we now have a complete model of long-term insect-pathogen dynamics. The pathogen is introduced into the host population each year by the contamination of egg masses, a process described by equations (4) and (5). When larvae hatching from these egg masses die, they produce pathogens that initiate an epidemic, a process described by equations (1) and (2), which ends because of host pupation. Larvae that are uninfected at the time of pupation survive to reproduce with fecundity  $\lambda$ . Before proceeding, however, we make explicit two additional assumptions. First, because there is little evidence that any infected gypsy moths survive (Murray et al. 1991), we assume that hosts that are infected but not yet dead when the epidemic ends also eventually die and so are converted to pathogen particles. Second, for now we assume that the distribution of host heterogeneity is the same at the beginning of each epidemic. In fact, we do not know how much of the variation is genetic or how rapidly the distribution may change under selection, but this assumption is a good starting point for understanding this complex system. We are currently collecting data to test this assumption, and we are developing models that relax it.

In what follows, we refer to the model in which epidemics are curtailed by host pupation as the “short-epidemic model.” Because this model can only be understood through extensive computer simulations, we also present a simpler model based on the infinite-epidemic equation that can be understood more fully than the short-epidemic model and can be simulated more

easily. This simpler model can be written as a set of difference equations:

$$N_{t+1} = \lambda N_t(1 - I), \quad (6)$$

$$Z_{t+1} = fN_tI + \gamma Z_\rho \quad (7)$$

$$1 - I = \left[ 1 + \frac{\bar{v}C^2}{\mu} (N_tI + \rho Z_t) \right]^{-1/C^2}. \quad (8)$$

Again,  $N_t$  and  $Z_t$  are the densities of hosts and pathogens in generation  $t$ . Equation (8) is essentially the infinite-epidemic equation (3) with the initial density of pathogens  $Z_t$ , scaled by  $\rho$ , the ratio of the mean susceptibility of hatching larvae to that of older larvae. In words, surviving hosts  $N_t(1 - I)$  produce on average  $\lambda$  offspring. Dead infected hosts  $N_tI$  are converted to infectious cadavers, of which a fraction  $f$  survive to infect egg masses in the following season, with relative susceptibility  $\rho$ . A fraction  $\gamma$  of infectious cadavers from previous generations survives from one season to the next. We thus allow pathogens that survive from one generation to the next to have a different survival rate than pathogens produced during the epidemic, but in accord with our anecdotal field observations, in what follows, we often assume that this survival rate  $\gamma$  is 0. This assumption has little effect on our results.

### Qualitative Dynamics of the Long-Term Models

Rescaling host and pathogen densities shows that the dynamics of both of our models depend only on fecundity  $\lambda$ , heterogeneity in susceptibility  $C$ , long-term virus survival  $\gamma$ , and a new parameter  $\phi$ , the expected infectiousness in the next generation of a particle produced in the current epidemic (app. A). The mean transmission rate  $\bar{v}$  and the pathogen decay rate  $\mu$  affect only mean host and pathogen densities. High  $\mu$  and low  $\bar{v}$  give high average host and pathogen densities, and vice versa. We define  $\phi \equiv f\rho$  so that  $\phi$  is the product of the probability  $f$  that a pathogen particle survives the interepidemic period times the relative mean susceptibility of newly hatched larvae  $\rho$ . Because newly hatched larvae have relatively high mean susceptibility,  $\rho$  is likely to be  $>1$ , so it is possible that  $\phi$  is  $>1$ . As we will discuss, this possibility is critical for understanding the dynamics of forest insects. The resulting rescaled model is

$$N_{t+1} = \lambda N_t(1 - I), \quad (9)$$

$$Z_{t+1} = \phi N_tI + \gamma Z_\rho \quad (10)$$

$$1 - I = [1 + C^2(N_tI + Z_t)]^{-1/C^2}. \quad (11)$$

Like many discrete-generation models, equations (9)–(11)

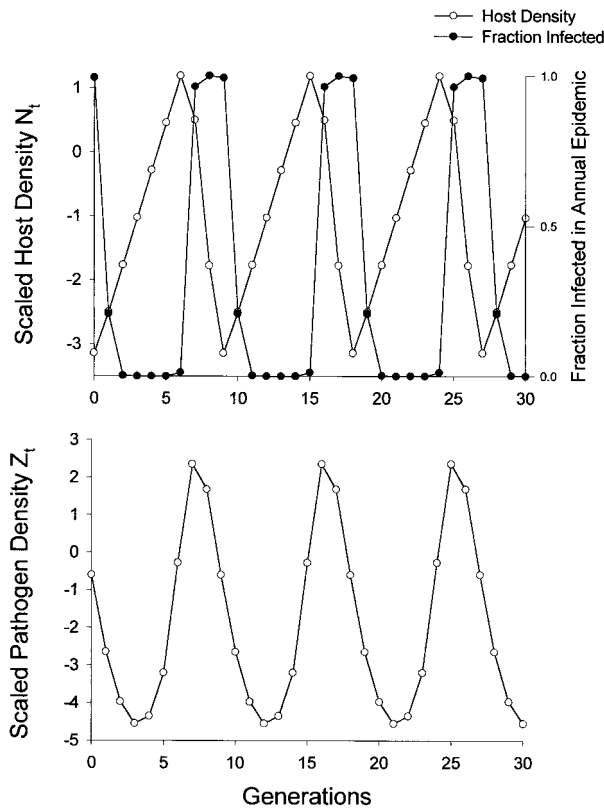


**Figure 2:** Long-term dynamics of the model for realistic parameter values ( $\lambda = 5.5$ ,  $C = 0.86$ ,  $\phi = 15$ ). Host outbreaks occur at 9-yr intervals and are terminated by a succession of pathogen epidemics. This pattern matches the dynamics of the gypsy moth and its virus.

can show chaotic dynamics, but chaos only occurs for unrealistically high values of fecundity ( $\lambda \geq 10,000$ ). For more realistic values of fecundity, equations (9)–(11) can show cycles that range in period from two generations to  $>20$  generations. Because of our interest in the dynamics of forest defoliators, we concentrate on parameter values that give realistic cycles with a period of five generations or more (fig. 2). We postpone a discussion of shorter-period fluctuations for a subsequent article.

An important advantage of the infinite-epidemic approximation is that we can derive expressions for the boundaries between stability and cycles for the infinite-epidemic model. Figure 3 shows these boundaries, and demonstrates the stabilizing effects of high heterogeneity  $C$ , high multiseason pathogen carryover  $\gamma$ , low fecundity  $\lambda$ , and low single-season pathogen carryover rate  $\phi$ . We note, however, that for  $\phi$  sufficiently small, the model shows the high-frequency oscillations associated with period doubling, which we do not consider here. The stabilizing effects of heterogeneity  $C$  are particularly strong,

such that high values can guarantee stability irrespective of the value of  $\lambda$ . Specifically, limit cycles cannot occur if  $C^2 > (\phi - \gamma)/(\phi - \gamma + 1)$  (app. B). Stability thus increases with increases in the squared coefficient of variation  $C$  of the distribution of susceptibility and is guaranteed if  $C^2 > 1$ . For lower levels of heterogeneity, cycles are more likely if  $\phi$  is large relative to  $\gamma$ .

The biology of these patterns is best understood in terms of single epidemics. Figure 1 shows that high levels of infection occur either when initial host density is above the epidemic threshold  $N_T$  or when there is a high initial density of pathogens. Limit cycles then occur when it takes several generations for the pathogen to reach densities high enough to suppress the host population, but suppression continues for one or more additional generations. This occurs when the pathogen carryover parameter  $\phi$  is higher

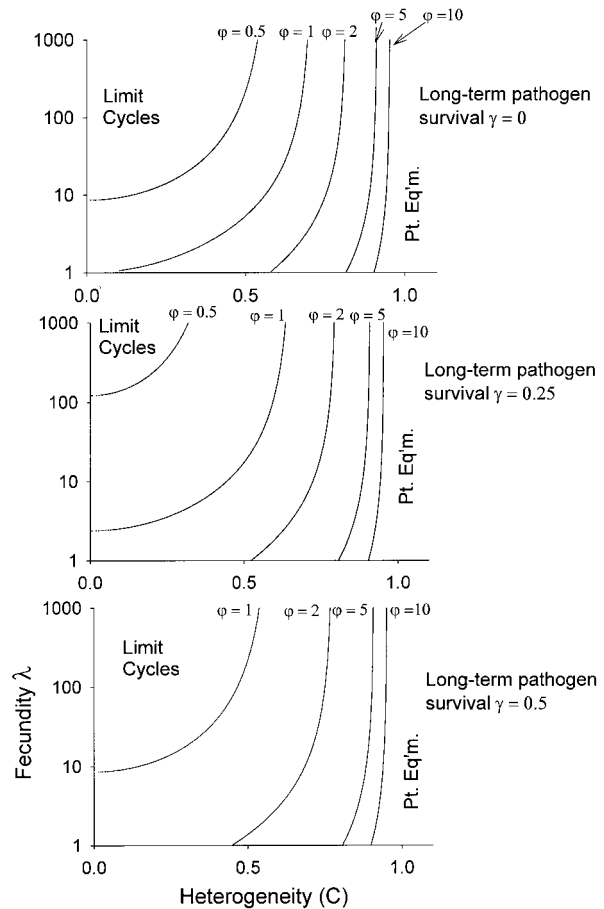


**Figure 3:** Ranges of parameter values for which limit-cycle bifurcations occur for the model with infinite epidemics, equations (9)–(11). Stability is promoted by high values of multigeneration pathogen carryover  $\gamma$ , low values of fecundity  $\lambda$ , high values of host heterogeneity  $C$ , and low values of current-generation pathogen carryover  $\phi$ .

so that newly hatched larvae have high relative susceptibility and/or pathogens produced in the epidemic have high overwinter survival. High values of the between-generation pathogen survival rate  $\gamma$ , however, lead to stability because, when there is a consistently high density of pathogens, disease incidence is always high enough to cause at least a moderate epidemic, and the population never overshoots the disease threshold. Finally, host heterogeneity in susceptibility  $C$  is strongly stabilizing because, as figure 1 shows, higher heterogeneity reduces the intensity of epidemics. As heterogeneity increases, each year's epidemic therefore reduces the population to near the disease threshold rather than well below it, which eliminates the overshooting phenomenon responsible for fluctuations.

The boundaries between stability and cycles are very similar for the short-epidemic model (not shown), and the discrepancy declines with increasing values of pathogen carryover  $\phi$  because high values of  $\phi$  lead to epidemics that rapidly burn out. For values of  $\phi \geq 5$ , the boundary between stability and cycles for the short-epidemic model is indistinguishable from that of the infinite-epidemic model. An important difference between the two models, however, is that the model with short epidemics is more likely to show unstable cycles, for which the amplitude of the cycles becomes larger and larger over time. Indeed, as heterogeneity  $C$  is reduced, we eventually reach a value of  $C$  at which the short-epidemic model is apparently unstable (meaning that peak densities grow to unbounded values) for all values of  $\lambda$ . In figure 4, we show the range of values of  $\phi$  and  $C$  for which the model is unstable irrespective of  $\lambda$ , for different values of epidemic length  $T$ . Figure 4 thus shows that moderate levels of heterogeneity prevent unstable limit cycles in the short-epidemic model, with  $C^2 > 1/2$  being sufficient to guarantee stable cycles (the infinite-epidemic model also shows these dynamics but only for very low levels of heterogeneity). These effects occur because shorter epidemic periods exacerbate the overshooting phenomenon that leads to stable limit cycles in the first place, and the effect becomes stronger as the epidemic length is shortened. This sort of instability is of course unrealistic; in real populations some sort of density dependence will act to keep populations bounded. Nevertheless, figure 4 is interesting because it shows that moderate levels of heterogeneity can have a stabilizing effect on outbreak dynamics.

#### Outbreaks in Defoliators: from Experiments to Time Series

In this section, we explore the consequences of our experimental estimates of heterogeneity  $C$  for gypsy moth population dynamics. Gypsy moth populations show moderate to high levels of heterogeneity in susceptibility

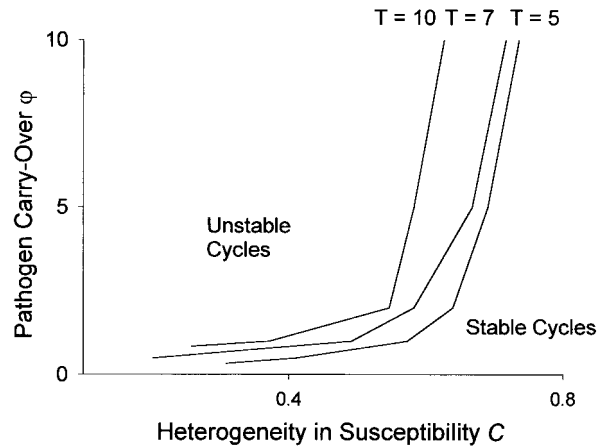


Figure 4: Effects of epidemic length on model stability, demonstrating that host heterogeneity in susceptibility plays a key role in stabilizing cycles in the short-epidemic model.

(Dwyer et al. 1997), and the model shows that high levels of heterogeneity are stabilizing, but gypsy moths in North America have unstable population dynamics (Williams and Leibhold 1995; Ostfeld et al. 1996). We therefore ask, Can our experimental data be reconciled with the unstable population dynamics of the gypsy moth? In particular, is the heterogeneity in susceptibility that we observed in our experiments so high that it would lead to stable equilibrium gypsy moth densities rather than outbreaks? Conversely, are the levels of heterogeneity in our data high enough to give stable cycles in the model, so that it is at least possible that populations are primarily regulated by disease alone?

An important preliminary question is, What constitutes outbreaking population dynamics? We will use the popular criterion of large-amplitude fluctuations in population density (Mattson et al. 1991). In our model, for reasonable parameter values, large-amplitude fluctuations always occur in the form of long-period limit cycles. The statistical evidence for cyclicity in time series of outbreaking gypsy moth populations is mixed (Williams and Leibhold 1995), however, so we are implicitly assuming that in many cases the underlying cyclicity is obscured by environmental stochasticity. In future work, we will explore this point further. A second key point is that we define cycle period to be the number of generations between peaks of host density, rather than trying to calculate when or whether populations return exactly to previous values (a peak in density is defined to occur when a year's density is higher than the preceding year's and the following year's densities). Clearly, the former definition is a more ecologically meaningful measure of cycle length. This kind of definition can be problematic with noisy or chaotic data; fortunately,

**Table 1:** Mean transmission rate and coefficient of variation of susceptibility derived by fitting the short-epidemic model to data collected at different scales

Source of data	Scales	Transmission $\bar{\nu}$ m <sup>2</sup> /d	Heterogeneity $C$	95% bounds on $C$
Field experiments	.1 m <sup>2</sup> , 1 wk			
Feral strain:				
1994	...	.36	.90	.002, 1.70
1995	...	.90	1.60	.81, 4.94
1996	...	3.37	1.44	.75, 4.22
Lab strain:				
1994	...	1.07	.81	.001, 1.66
1995	...	1.94	1.00	.002, 1.65
1996	...	2.11	.77	.24, .83
Natural epidemics	4–9 ha, 7–9 wk	.54	.59	...
Time series	.16 ha, 15 yr	2.68	.86	...

Note: Epidemic data were collected by Woods and Elkinton (1987) from single epidemics in four naturally occurring populations, and the model was fit to the entire epidemic time series by minimizing the sum of squares between the model and the weekly data. Experimental data were collected by Dwyer et al. (1997) from transmission experiments using either “feral-strain” or “lab-strain” larvae (see text for details) on single oak branches, and the model was fit to the fraction of larvae becoming infected in each bag. Dwyer et al. (1997) describe these fitting procedures in greater detail. Time series data are as depicted in figure 6 and were collected from 20 78.5-m<sup>2</sup> plots (Ostfeld et al. 1996). To calculate mean transmission  $\bar{\nu}$  from the time series data, we converted from egg masses per hectare to larvae per hectare assuming 250 eggs per egg mass and a leaf area index of 1.4 (Dwyer and Elkinton 1993). The main text gives further details on our methods of fitting the model to these long-term data;  $\bar{\nu}$  = mean transmission rate,  $C$  = coefficient of variation of susceptibility, with  $\mu$  taken from Dwyer et al. (1997).

some gypsy moth time series show clearly defined peaks and troughs, as does our model in the relevant parameter ranges. Also, in this section, we are concerned with quantitative model dynamics, so we focus exclusively on the short-epidemic model on the grounds that it is likely to provide a more precise description of gypsy moth dynamics.

With these points in mind, we can use the model to assess the implications of our transmission data (Dwyer et al. 1997), which were generated by exposing groups of 25 larvae to different densities of virus on single oak branches in the field. An important detail is that our experiments quantified heterogeneity for two different strains of the insect that differed greatly in levels of heterogeneity. Larvae of the “feral” strain came from eggs mixed together from feral populations scattered across the states of Massachusetts, New Hampshire, and West Virginia and showed high heterogeneity, whereas larvae of the “lab” strain came from a laboratory colony that has been maintained for >40 generations and showed low heterogeneity. The feral strain was thus constructed to be as heterogeneous as possible, while the lab strain was intentionally chosen to show lower heterogeneity. The lab larvae were nevertheless fairly heterogeneous, so we suspect that naturally occurring feral larvae from single populations would show levels of heterogeneity intermediate between these two strains.

Given this caveat, the model shows that the estimates of heterogeneity  $C$  from our data do not preclude the

possibility of cycles, in that point estimates from the lab populations are all  $\leq 1$  (table 1). These estimates, however, have confidence intervals that are large relative to the region of parameter space in which cycles occur. To show this, we bootstrapped 10,000 estimates of heterogeneity  $C$  for each larval strain in each of 2 yr of experiments (the third year had low replication), by making eight random draws with replacement from our eight replicates 10,000 times, and then fitting a reduced version of equations (1) and (2) to each draw (see Dwyer et al. 1997 for more details). This procedure showed that, for the lab-strain larvae, nearly all of the bootstraps of the 1996 data (99.96%) and more than half of the bootstraps of the 1995 data (52.5%) were  $< 1$ . For the feral larvae, 13% of the bootstraps of the 1996 data and 4.3% of the bootstraps of the 1995 data were  $< 1$ . In other words, only one of the feral-strain data sets, and neither of the lab-strain data sets, can reject the hypothesis of stable cycles. On the other hand, because nearly half of the bootstraps of the 1995 lab-strain data are  $> 1$ , that data set cannot reject the hypothesis of a stable equilibrium either. Also, 15% of bootstraps of the 1996 lab-strain data gave levels of heterogeneity  $C < 0.6$ , and as figure 5 shows,  $C < 0.6$  is low enough to almost always permit unstable cycles. In other words, our data are too noisy relative to the range of parameters that gives stable cycles to single out stable cycles as the only realistic outcome of the model. Nevertheless, it is surprising that our data cannot reject the hypothesis



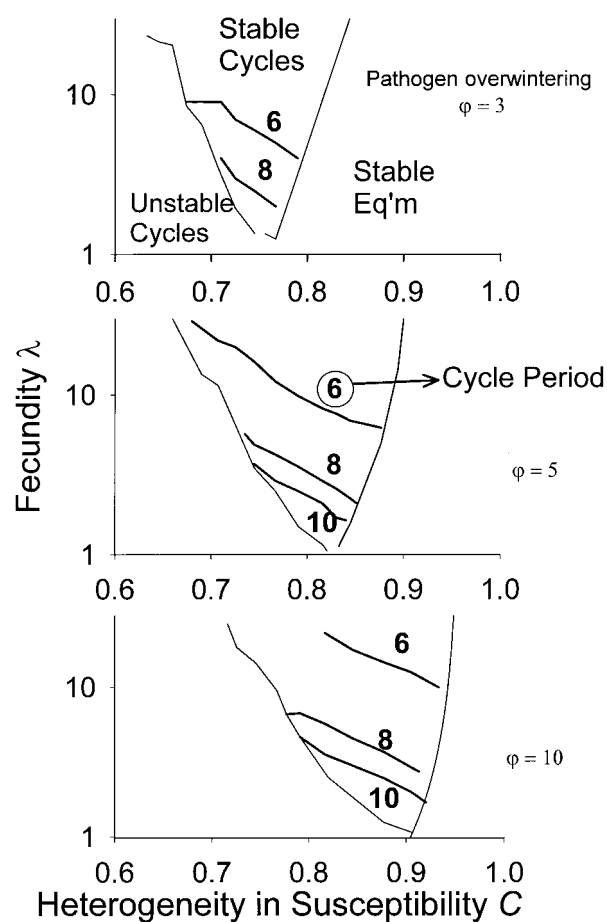


Figure 5: Cycle periodicity and the parameter range that permits stable cycles for the short-epidemic model. The cycle period and the chance of unstable cycles both increase as fecundity  $\lambda$  decreases.

of stable cycles given the high levels of heterogeneity in susceptibility in the data.

Given that our transmission data do not preclude the possibility of outbreaks, we also compare the model to gypsy moth population data more quantitatively. Specifically, gypsy moth populations typically fluctuate over about four orders of magnitude in density (Elkinton and Liebhold 1990), and so we ask, Does the model show this amplitude of fluctuations for realistic parameter values? We define amplitude to mean the difference in density between peaks and troughs of the population cycle. Figure 5 shows that cycle period increases with increasing values of pathogen carryover  $\phi$  and decreasing values of fecundity  $\lambda$  and heterogeneity in susceptibility  $C$ , matching the effects of these parameters on the boundary between limit cycles and a stable equilibrium. Figure 5 also shows that the model can match the observed 9-yr period of gypsy moth population fluctuations for a broad range of param-

eter values. The further requirement of an amplitude of fluctuation of about four orders of magnitude, however, means that fecundity  $\lambda$  must be about 5 (not shown). Here, “fecundity” is interpreted to mean “net population change in the near-absence of the disease” rather than “eggs per egg mass” (Hassell et al. 1976). Under this definition, observed net gypsy moth fecundity  $\lambda$  is about 11 (Elkinton et al. 1996). Given that the variance in net gypsy moth fecundity from year to year is large ( $SE = 9.1, n = 8$ ), model and data are in approximate agreement.

More quantitatively, in figure 6, we show the best fit of the model to a time series for gypsy moth (Ostfeld et al. 1996). By first transforming the data according to  $\log_e [N_{t+1}/N_t]$  (Turchin and Taylor 1992), we were able to fit the nondimensionalized short-epidemic model to the data using only fecundity  $\lambda$ , heterogeneity  $C$ , and pathogen survival  $\phi$  (app. A; note that we assume  $\gamma = 0$ ). We found the best-fit values of these parameters by calculating the sum of the squared differences between the model and the data for parameter combinations that spanned the area of parameter space in which the model shows stable cycles. To generate the figure, we then used the model output for the best-fit values of the parameters and varied the ratio  $\bar{\nu}/\mu$  until we had achieved a good fit between the host density predicted by the model and the host density in the data (app. A), as determined again by least squares. Although this time series is short and is based on a sampling area of only 0.16 ha (in particular the low points of each cycle are based on very small sample sizes; Ostfeld et al. 1997), nevertheless, figure 6 demonstrates that the model does a good job of reproducing the data. Also, estimates

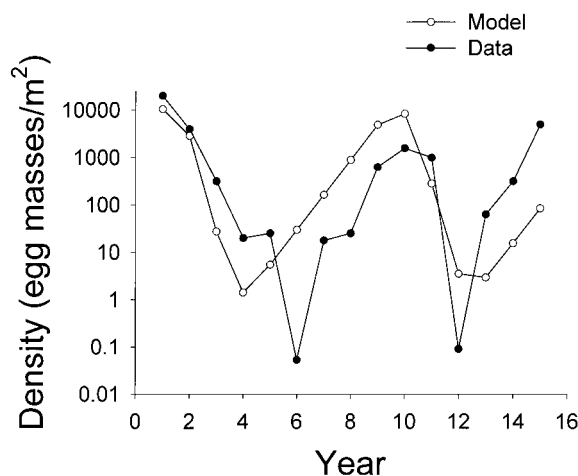


Figure 6: Best fit of the short-epidemic model to time series data for gypsy moth *Lymantria dispar* (Ostfeld et al. 1996). Parameter values are fecundity  $\lambda = 5.5$ , heterogeneity in susceptibility  $C = 0.86$ , and pathogen overwinter survival  $\phi = 15$ . Table 1 gives the value of  $\bar{\nu}$ .

of mean transmission  $\bar{\nu}$  and heterogeneity  $C$  from these data are close to the parameters estimated both from our experimental data and from single epidemics (table 1).

### Discussion

Our work has led us to a general conclusion that is identical to that of Anderson and May's (1981) work, that host-pathogen interactions are likely to cause outbreaks in forest-insect populations. Our models include realistic features of insect-pathogen interactions that are missing from Anderson and May's models, however, and this additional realism leads us to different conclusions about which biological details are important in driving outbreaks. Specifically, Anderson and May emphasized the importance of high pathogen survival in causing long-period cycles, but our models have shown instead that cycles are possible even with relatively low pathogen survival because of the high average susceptibility of early stage larvae relative to later-stage larvae. Also, Anderson and May used continuous-generation host-pathogen models; because the simplest such models give stable population dynamics, a major thrust of their work was that the long-lived infectious stage, typical of insect pathogens, destabilizes their models enough to give long-period cycles. In contrast, because our models realistically assume discrete host generations, they are likely to show unstable dynamics. Consequently, we instead emphasize a mechanism that stabilizes what would otherwise be unstable cycles, specifically, host heterogeneity in susceptibility. In this respect, discrete-generation host-pathogen models are more like discrete-generation host-parasitoid models (Hassell et al. 1991), a point first made by Briggs and Godfray (1996).

The differences between our conclusions and those of Anderson and May are due to differences in model structure for which our gypsy moth data provide strong support. First, our experimental data strongly support the inclusion of host heterogeneity in susceptibility and delays between infection and death in our epidemic model equations (1) and (2) (Dwyer et al. 1997). Second, discrete host generations are an obvious feature of gypsy moth populations, and the experiments of Murray and Elkinton (1989, 1990) have made clear the importance of virus contamination of egg masses for the initiation of epidemics. Breaking the gypsy moth life cycle into epidemic and interepidemic periods is therefore a crucial feature of our model. This structure is further supported by the ability of the models to accurately describe the dynamics of gypsy moth populations at spatial scales of entire regions and over timescales of decades (figs. 5, 6). In particular, our estimates of the average transmission rate  $\bar{\nu}$  and of host heterogeneity in susceptibility  $C$  from long-term data are

similar to estimates from short-term experiments (table 1).

Comparison of our model to the model of Briggs and Godfray (1996) suggests that host heterogeneity in susceptibility is an especially important detail. Briggs and Godfray's main model is similar to ours in allowing for discrete host generations and a single epidemic each year. A major difference, however, is that instead of explicitly incorporating a distribution of host heterogeneity in susceptibility, they incorporate a kind of phenomenological heterogeneity in transmission, following a formulation used in host-parasitoid models. In the resulting model, cycles are only found for a very narrow range of parameters, unless long-term pathogen survival is allowed. Our model most closely matches Briggs and Godfray's main model if we set single-generation pathogen carryover  $\phi \leq 1$  and long-term pathogen survival  $\gamma = 0$ . For these parameter values, however, our model produces cycles for a broad range of values of fecundity  $\lambda$  and host heterogeneity  $C$ . Even when Briggs and Godfray allowed for long-term pathogen survival ( $\gamma > 0$ ), the period of the cycles apparently never exceeded four generations. These differences suggest that host heterogeneity in susceptibility is of profound importance for the dynamics of insect-pathogen interactions and that the details of how heterogeneity is incorporated matter a great deal. For the particular case of host heterogeneity in susceptibility, our results suggest that a mechanistic approach is crucial.

Our data, however, suggest some caveats. First, the short-epidemic model shows that the levels of heterogeneity in susceptibility that we observe in our data are likely to stabilize what might otherwise be unstable cycles, but the confidence intervals on our data are large enough that the importance of heterogeneity in susceptibility in leading to stable cycles is an open question. In particular, Bonsall et al. (1999) showed that adding nondisease direct density dependence to Briggs and Godfray's (1996) host-pathogen model also tends to stabilize unstable cycles. Because this direct density dependence is typical of gypsy moth populations at high density (Carter et al. 1991), the work of Bonsall et al. (1999) suggests that both host heterogeneity and competition for food act to stabilize disease-driven fluctuations in gypsy moth populations. In fact, there is at least a short list of other biological details of gypsy moth population dynamics that are missing from our model but that are known to be important in gypsy moth population dynamics. Indeed, low-density gypsy moth populations may be kept in check by density-dependent small-mammal predation (Elkinton and Liebhold 1990). Evidence for such density dependence is equivocal (Elkinton et al. 1996), but evidence for the importance of small-mammal predation on late instars and pupae, especially by the white-footed mouse *Peromyscus leucopus*, is strong. Changes in low-

density gypsy moth populations are strongly correlated with changes in densities of white-footed mice (Elkinton et al. 1996; Ostfeld et al. 1996), and experimental removals of small mammals lead to sharp increases in gypsy moth populations (Jones et al. 1998). The major food of white-footed mice, however, is acorns. Consequently, changes in mouse population densities are strongly correlated with changes in the acorn crop (Elkinton et al. 1996; Ostfeld et al. 1996), and experimental additions of acorns can prevent increases in gypsy moth populations (Jones et al. 1997). Because the acorn crop depends in turn on regional weather patterns, the strongest overall effect of small-mammal predation on gypsy moth population dynamics may be that it introduces variability in gypsy moth net fecundity at low density. In particular, several successive years of poor acorn crops lead to collapses in small mammal populations that allow gypsy moth populations to grow to densities at which small-mammal predation is insignificant. Such populations eventually reach the high densities at which virus epidemics occur. This variability may explain some of the fluctuations seen in time series of gypsy moth defoliation data (Williams and Liebhold 1995) and may affect the periodicity and stability of the fluctuations in our models. An important future direction for modeling gypsy moth population dynamics is thus to include small-mammal predation and environmental stochasticity. Likewise, quantitative application of our models to the dynamics of other forest insects may require other biological details. Western tent caterpillars, for example, experience reduced fecundity due to the exposure of larvae to low doses of virus (Rothman and Myers 1994), an effect that does not occur in gypsy moths (Murray et al. 1991). We therefore echo calls for models that investigate multiple factors in insect population dynamics (Bowers et al. 1993; Hunter and Dwyer 1998).

It is important to emphasize, however, that the dynamics of the gypsy moth and other outbreaking insects may be less complicated than is sometimes believed. For example, recent data suggest that maternal effects (Myers et al. 1999; M. Erelli, personal communication) and induced host-plant defenses (D'Amico et al. 1998) may have little effect on gypsy moth population dynamics. A major point of our work is thus to illustrate the usefulness of simple models. Indeed, the infinite-epidemic model tells us much of what we need to know about the short-epidemic model, yet the former can be analyzed mathematically and so understood more deeply than the latter, which can only be simulated. In fact, our infinite-epidemic model was inspired by May's (1981) model, which makes the additional assumption that the yearly epidemic is begun by an infinitesimally small density of pathogens. Simple models can thus be at least as useful as giant simulation models in understanding host-pathogen dynamics (Onstad et al.

1990) and have the advantage of being more easily understood.

### Acknowledgments

We thank C. H. J. Godfray, E. Holmes, W. F. Morris, A. F. Hunter, and K. L. S. Drury for commenting on earlier versions of the manuscript. Our research was supported by National Science Foundation (NSF) grant DEB-97-07610 to S.A.L. and G.D., who was also supported by a Dropkin Fellowship awarded by the University of Chicago and two earlier NSF grants awarded to G.D. and J.S.E. G.D. thanks J. M. Bergelson and the NSF for shelter from the storm, C. Styles for navigational assistance during the storm, and A. F. Hunter for a reason to endure the storm.

## APPENDIX A

### Derivation of the Infinite-Epidemic Equation

In this appendix, we derive equations (4) and (5), which give the initial conditions at the start of the epidemic, and we derive the infinite-epidemic equation (8) (of which eq. [3] is a special case).

### The Egg-Mass Infection Process

As we discuss in the main text, our assumption is that the process by which hatching larvae become infected is essentially identical to the process by which larvae become infected later in the season. We therefore model it using the equations

$$\frac{\partial S}{\partial t} = -\eta \nu S Z_\nu \quad (\text{A1})$$

$$\frac{dP}{dt} = \eta Z_\nu \int_0^\infty \nu S(\nu, t) d\nu, \quad (\text{A2})$$

where  $\eta$  is the susceptibility of hatching larvae relative to the susceptibility of larvae later in the season. For simplicity, here we assume that overwintering pathogens can infect egg masses for some fixed period of time, say, of length  $\hat{t}$ . Integrating equations (A1) and (A2) from 0 to  $\hat{t}$  gives equations (4) and (5) in the main text, with the definition  $\rho \equiv \eta \hat{t}$ . Allowing for alternative assumptions about the length of time for which egg masses are exposed and the pathogen is infectious is not difficult; a constant rate of breakdown  $\theta$  of the pathogen, for example, gives  $\rho \equiv \eta(1 - e^{-\theta \hat{t}})$ . Because we do not expect to be able to distinguish among these processes, in the main text we introduce only the aggregate parameter  $\rho$  that allows for

differences in both mean susceptibility and in length of the exposure period.

**The Infinite Epidemic I: Force of Infection and Gamma-Distributed Susceptibility**

Next, we derive the infinite-epidemic equation (6) by allowing  $t \rightarrow \infty$  in equations (1) and (2) (see Kermack and McKendrick 1927, for a similar analysis, and Metz and Diekmann 1986, for an extension of Kermack and McKendrick’s approach). We start by integrating equation (1) to obtain

$$\log \frac{S(\nu, \infty)}{S(\nu, 0)} = -\nu \int_0^\infty P(t) dt. \tag{A3}$$

For convenience in what follows, we define the force of infection over the course of the epidemic,  $F \equiv \int_0^\infty P(t) dt$ , so that our next step is to find an expression for  $F$ . The simplest way to do this is to observe that the force of infection arises either from new infections or from cadavers produced in previous generations ( $Z_i$ ). If we then define  $L_1$  to be the average infectious lifespan of cadavers arising from new infections and  $L_2$  to be the average infectious lifespan of cadavers that were produced in previous generations, we have

$$F = L_1[\hat{S}(0) - \hat{S}(\infty)] + L_2 Z_i. \tag{A4}$$

Alternatively, we can follow Kermack and McKendrick’s (1927) approach. To do this, we first generalize equations (1) and (2). Specifically, we define the distribution of times between infection and infectiousness to be  $f(a)$ , the survival probability function for infectious cadavers produced during the epidemic to be  $l_1(a)$ , and the survival probability function for cadavers present from the beginning of the epidemic to be  $l_2(a)$ , where  $a$  is the age of the infection or the age of the infectious particle, respectively. Then, if we let  $i(t)$  be the rate of production of new infections at time  $t$ , we can write an expression for the force of infection over the course of the epidemic:

$$F = \int_0^\infty \int_0^t i(\theta) \int_\theta^t f(r - \theta) l_1(t - r) dr d\theta dt + Z_i \int_0^\infty l_2(t) dt. \tag{A5}$$

The first integral on the right-hand side of equation (A5) is a sum of terms that gives the cadavers contributed by individuals that were infected at time  $\theta$ , became infectious at time  $r$ , and then remained infectious until time  $t$ . If we

then follow Kermack and McKendrick by rearranging the order of integration and making several substitutions, and so forth, we again arrive at our force of infection equation (A4). Note that equation (A4) makes no assumptions about the distribution of times between infection and death or about the distribution of the lifetimes (breakdown rates plus translocation rates) of infectious cadavers. Equation (A4) is therefore also a limiting case of the short-epidemic model.

Next, we combine equation (A3) with equation (A4) to get

$$\log \frac{S(\nu, \infty)}{S(\nu, 0)} = -\nu \{L_1[\hat{S}(0) - \hat{S}(\infty)] + Z_i L_2\}. \tag{A6}$$

To finish the derivation, we assume that heterogeneity in susceptibility is gamma distributed with mean  $\bar{\nu}$  and squared coefficient of variation  $V$ . If  $\hat{S}(t)$  is the total host population density at time  $t$  during the epidemic, we can integrate equation (A6) to obtain

$$\hat{S}(\infty) = \hat{S}(0) [1 + V \bar{\nu} \{L_1[\hat{S}(0) - \hat{S}(\infty)] + Z_i L_2\}]^{-1/V} \tag{A7}$$

Substituting  $1 - I$  for  $\hat{S}(\infty)/\hat{S}(0)$ , and recalling that in generation  $t$   $\hat{S}(0) \equiv N_p$ , gives an implicit expression for the proportion of the population infected in the epidemic:

$$1 - I = [1 + V \bar{\nu} (L_1 N_p I + \rho L_2 Z_i)]^{-1/V}. \tag{A8}$$

In the main text, we further substitute the coefficient of variation  $C^2 = V$ , and we assume that the breakdown rates of current-generation and previous-generation cadavers are the same, so that  $L_1 \equiv L_2 \equiv 1/\mu$ .

Because the left-hand side of equation (A8) goes from 1 to 0 as  $I$  goes from 0 to 1, while the right-hand side remains between 0 and 1, it is clear that the equation must have a root. Because the second derivative of the right-hand side can be shown to be everywhere positive, and since the curve given by the right-hand side crosses the straight line given by the left-hand side from below to above, this solution must be unique.

**The Infinite Epidemic II: A Distribution-Free Approach Using Moment Closure**

It happens that the assumption of gamma-distributed susceptibility is not strictly necessary to derive equation (A8). To show this, we use an approximation method introduced by Dushoff (1999), in which one reduces a partial differential equation to a set of ordinary differential equations for the moments of the distribution of susceptibility in the host population. We first define

$$S_j = \int_0^\infty \nu^j S(\nu, t) d\nu, \quad (\text{A9})$$

where  $S_j$  is the  $j$ th moment of the distribution of susceptibility. Differentiating equation (A9) with respect to time and substituting from equation (1) gives

$$\frac{dS_j}{dt} = -PS_{j+1}. \quad (\text{A10})$$

It is convenient to define  $m_j \equiv S_j/S_0$ . In particular,  $m \equiv m_1$  is the mean of the distribution of host susceptibility. By the quotient rule of differentiation, we then have

$$\frac{dm_j}{dt} = -P(m_{j+1} - mm_j). \quad (\text{A11})$$

We have now replaced the partial differential equation (1) with a set of ordinary differential equations in terms of the moments of the distribution of susceptibility. The remaining problem is that, as the moment equation (A11) shows, the rate of change of each moment depends on the next higher moment, so that we must approximate the higher-order moments.

We construct an approximation by assuming that the coefficient of variation of the distribution of susceptibility remains constant, so that we need keep track of only the first two moments of the distribution. This means that, if  $V$  is again the squared coefficient of variation, we have

$$\frac{m_2 - m^2}{m^2} = V, \quad (\text{A12})$$

so that we have

$$\frac{dm}{dt} = -VPm^2, \quad (\text{A13})$$

$$\frac{d\hat{S}}{dt} = -mP\hat{S}, \quad (\text{A14})$$

where total population density  $\hat{S}(t) \equiv S_0(t)$

Surprisingly, the orbits of this system can be found explicitly. Divide equation (A13) by equation (A14) and integrate from 0 to  $t$ , to arrive at

$$m = \bar{\nu} \left[ \frac{\hat{S}(t)}{\hat{S}(0)} \right]^V, \quad (\text{A15})$$

recalling that the mean at time 0  $m(0)$  is just the distribution mean  $\bar{\nu}$ .

We now substitute equation (A15) into equation (A14) to get

$$\frac{d\hat{S}}{dt} = -\bar{\nu} \left[ \frac{\hat{S}(t)}{\hat{S}(0)} \right]^V P\hat{S}. \quad (\text{A16})$$

Rearranging gives

$$\frac{d\hat{S}}{\hat{S}(t)^{V+1}} = -\frac{\bar{\nu}}{\hat{S}(0)^V} P dt. \quad (\text{A17})$$

Now we can integrate over  $t$  from 0 to  $\infty$  to get

$$\hat{S}(0)^{-V} - \hat{S}(\infty)^{-V} = -\frac{\bar{\nu}}{\hat{S}(0)^V} F, \quad (\text{A18})$$

where  $F$  is the total force of infection, as above. Rearranging, substituting for  $F$ , and substituting  $I$  for the fraction infected at the end of the epidemic again gives equation (A8).

### Rescaling

To rescale the infinite-epidemic model, we divide host densities  $N_t$  and pathogen densities  $Z_t$  by the epidemic threshold  $N_T \equiv \mu/\bar{\nu}$ , which gives the nondimensionalized equations (9)–(11). Our simulations of the short-epidemic model rely on the moment-closure techniques described above. Equations (A1) and (A2) then become

$$\frac{d\hat{S}}{dt} = -\rho \bar{\nu} Z_t \hat{S}(t) \left[ \frac{\hat{S}(t)}{N_t} \right]^V, \quad (\text{A19})$$

$$\frac{dP}{dt} = \bar{\nu} Z_t \hat{S}(t - \tau) \left[ \frac{\hat{S}(t - \tau)}{N_t} \right]^V. \quad (\text{A20})$$

Equations (1) and (2) become

$$\frac{d\hat{S}}{dt} = -\bar{\nu} P \hat{S} \left[ \frac{\hat{S}(t)}{N_t} \right]^V, \quad (\text{A21})$$

$$\frac{dP}{dt} = \bar{\nu} P(t - \tau) \hat{S}(t - \tau) \left[ \frac{\hat{S}(t - \tau)}{N_t} \right]^V - \mu P. \quad (\text{A22})$$

The short-epidemic model is then

$$N_{t+1} = \lambda N_t (1 - I), \quad (\text{A23})$$

$$Z_{t+1} = f N_t I + \gamma Z_t, \quad (\text{A24})$$

where  $I = [\hat{S}(T) - \hat{S}(0)]$  and  $T$  is the length of the epidemic. We can then rescale as before.

APPENDIX B

Qualitative Analysis of the Infinite-Epidemic Model

In this appendix, we analyze the infinite-epidemic model, equations (9)–(11), which are the nondimensionalized version of equations (6)–(8). We derive an expression for the boundary between a stable equilibrium and limit cycles, and we show that the squared coefficient of variation of the distribution of susceptibility  $C^2 > 1$  guarantees stability of the model against limit cycles (we have also shown that  $C^2 > 1/2$  guarantees stability against flip bifurcations, but we omit the proof in the interests of brevity).

We begin by observing that the trivial equilibrium  $\bar{N} = 0, \bar{Z} = 0$  is globally stable for all  $\lambda < 1$ . In what follows, we therefore restrict our attention to  $\lambda > 1$ .

Although taking a model step requires solution of the implicit equation (11), the nontrivial equilibrium can, remarkably, be written explicitly in terms of the parameters. From equation (11), we calculate the equilibrium value of  $I, \bar{I} = 1 - 1/\lambda$ . Then equation (10) gives  $\bar{Z}$  in terms of the parameters and  $\bar{N}$ , and we can substitute into equation (9) to find the equilibrium:

$$\begin{aligned} \bar{N} &= \frac{(\lambda^V - 1)(1 - \gamma)\lambda}{V(1 + \phi - \gamma)(\lambda - 1)}, \\ \bar{Z} &= \frac{\phi(\lambda^V - 1)}{V(1 + \phi - \gamma)}. \end{aligned} \tag{B1}$$

We can calculate the Jacobian matrix at the equilibrium (B1) by differentiating (9)–(11) with respect to  $N$  and  $Z$ , respectively:

$$\mathbf{J} = \begin{bmatrix} 1 - \lambda \bar{N} I_N & -\lambda \bar{N} I_Z \\ \phi \bar{I} + \phi \bar{N} I_N & \phi \bar{N} I_Z + \gamma \end{bmatrix}, \tag{B2}$$

where  $I_N$  and  $I_Z$  are the respective partial derivatives of  $I$  at the nontrivial equilibrium, which can be calculated by differentiating (11) and solving. Note that  $I_N = I_Z$ .

We analyze stability of the nontrivial equilibrium using the Jury criteria (Murray 1993). The equilibrium will be stable if and only if the determinant (det) and trace (tr) obey the inequalities:

$$|\text{tr}| - 1 < \text{det} < 1, \tag{B3}$$

with “flip” bifurcations leading to period doubling if the first inequality is violated and “Hopf” bifurcations leading to longer-period cycling if the second is violated with

$\text{tr} < 0$ . To investigate limit cycles, we examine the determinant. From the Jacobian (B2),

$$\text{det} = \gamma + I_p \bar{N}(\phi - \lambda\gamma\bar{I} - \lambda\phi\bar{I}). \tag{B4}$$

Substituting for  $\bar{N}, \bar{I}$ , and  $I_Z$  gives

$$\begin{aligned} \text{det} &= \gamma \\ &+ \frac{[\lambda(\phi - \gamma) + \gamma](1 - \gamma)(\lambda^V - 1)}{V\lambda^V(\lambda - 1)(1 + \phi - \gamma) - (1 - \gamma)(\lambda^V - 1)}. \end{aligned} \tag{B5}$$

When it is recalled that  $\gamma < 1$  and  $\lambda > 1$ , it can be shown that the denominator in equation (B5) is positive. Thus the stability criterion  $\text{det} < 1$  can be rearranged to give

$$\frac{\lambda^V - 1}{V\lambda^V} < \frac{(1 + \phi - \gamma)(\lambda - 1)}{\lambda(\phi - \gamma) + 1}. \tag{B6}$$

We now show that this criterion always holds when  $V > 1$ . The right-hand side can be shown to be a decreasing function of  $\eta \equiv \phi - \gamma$  and thus always greater than  $(\lambda - 1)/\lambda$ , the value it approaches as  $\eta \rightarrow \infty$ . The left-hand side is a decreasing function of  $V$  and is thus less than  $(\lambda - 1)/\lambda$ , whenever  $V > 1$ . Thus  $V > 1$  guarantees no limit cycles.

More generally, by taking the second derivative, we can show that the criterion is satisfied when  $\lambda$  is near 1 precisely when

$$V > \frac{\eta - 1}{\eta + 1}, \tag{B7}$$

where  $\eta \equiv \phi - \gamma$  is defined for convenience. Similarly, we can use L'Hôpital's rule to show that the criterion is satisfied when  $\lambda \rightarrow \infty$  if, and only if,

$$V > \frac{\eta}{\eta + 1}. \tag{B8}$$

Thus, when  $V > \eta/(\eta + 1)$ , the criterion (B6) holds both for  $\lambda \rightarrow 1$  and for  $\lambda \rightarrow \infty$ . We can in fact show that it holds for all  $\lambda$  and thus that there are no limit cycles when (B8) holds. When  $(\eta - 1)/(\eta + 1) < V < \eta/(\eta + 1)$ , (B6) holds for  $\lambda$  near 1, but not for large  $\lambda$ ; thus, there is a Hopf bifurcation at some value of  $\lambda$ . Finally, when  $V < (\eta - 1)/(\eta + 1)$  (which is possible only when  $\eta > 1$ ), (B6) does not hold for small or large  $\lambda$ . In fact, we can show that it is not true for any  $\lambda > 1$ , and that there is a “loop bifurcation” at  $\lambda = 1$  and thus cycles of very long period when  $\lambda$  is near 1.

## Literature Cited

- Anderson, R. M., and R. M. May. 1980. Infectious diseases and population-cycles of forest insects. *Science* (Washington, D.C.) 210:658–661.
- . 1981. The population dynamics of microparasites and their invertebrate hosts. *Philosophical Transactions of the Royal Society of London B, Biological Sciences* 291:451–524.
- Anderson, R. M., R. M. May, G. F. Medley, and A. Johnson. 1986. A preliminary study of the transmission dynamics of the (HIV), the causative agent of AIDS. *IMA Journal of Mathematics Applied in Medicine and Biology* 3: 229–263.
- Bonsall, M. B., H. C. J. Godfray, C. J. Briggs, and M. P. Hassell. 1999. Does host self-regulation increase the likelihood of insect-pathogen population cycles? *American Naturalist* 153:228–235.
- Bowers, R. G., M. Begon, D. E. Hodgkinson. 1993. Host-pathogen population cycles in forest insects: lessons from simple-models reconsidered. *Oikos* 67:529–538.
- Briggs, C. J., and H. C. J. Godfray. 1996. Dynamics of insect-pathogen interactions in seasonal environments. *Theoretical Population Biology* 50:149.
- Briggs, C. J., R. S. Hails, N. D. Barlow, and H. C. J. Godfray. 1995. The dynamics of insect-pathogen interactions. Pages 295–326 in B. T. Grenfell and A. P. Dobson, eds. *Ecology of infectious diseases in natural populations*. Cambridge University Press, Cambridge.
- Campbell, R. W. 1978. Some effects of gypsy moth density on rate of development, pupation time, and fecundity. *Annals of the Entomological Society of America* 71: 442–448.
- Carter, M. R., F. W. Ravlin, and M. L. McManus. 1991. Changes in gypsy-moth (Lepidoptera: Lymantriidae) fecundity and male wing length resulting from defoliation. *Environmental Entomology* 21:1308–1318.
- Cory, J. S., R. S. Hails, and S. M. Sait. 1997. Baculovirus ecology. Pages 301–340 in L. K. Miller, ed. *The baculoviruses*. Plenum, New York.
- D'Amico, V., and J. S. Elkinton. 1995. Rainfall effects on transmission of gypsy-moth (Lepidoptera: Lymantriidae) nuclear polyhedrosis-virus. *Environmental Entomology* 24:1144–1149.
- D'Amico, V., J. S. Elkinton, G. Dwyer, and J. P. Burand. 1996. Virus transmission in gypsy moths is not a simply mass-action process. *Ecology* 77:201–206.
- D'Amico, V., J. S. Elkinton, G. Dwyer, R. B. Willis, and M. E. Montgomery. 1998. Foliage damage does not affect within-season transmission of an insect virus. *Ecology* 79:1104–1110.
- Dushoff, J. 1999. Host heterogeneity and disease endemicity: a moment-based approach. *Theoretical Population Biology* 56:325–335.
- Dwyer, G. 1991. The effects of density, stage and spatial heterogeneity on the transmission of an insect virus. *Ecology* 72:559–574.
- Dwyer, G., and J. S. Elkinton. 1993. Using simple models to predict virus epizootics in gypsy moth populations. *Journal of Animal Ecology* 62:1–11.
- . 1995. Host dispersal and the spatial spread of insect pathogens. *Ecology* 76:1262–1275.
- Dwyer, G., J. S. Elkinton, and J. P. Buonaccorsi. 1997. Host heterogeneity in susceptibility and disease dynamics: tests of a mathematical model. *American Naturalist* 150: 685–707.
- Dwyer, G., J. Dushoff, J. S. Elkinton, J. P. Burand, and S. A. Levin. 2000. Host heterogeneity in susceptibility: lessons from an insect virus. In U. Dieckmann, ed. *Virulence management*. Springer, Berlin (in press).
- Elkinton, J. S., and A. M. Liebhold. 1990. Population dynamics of gypsy moth in North America. *Annual Review of Entomology* 35:571–596.
- Elkinton, J. S., W. M. Healy, J. P. Buonaccorsi, G. H. Boettner, A. M. Hazzard, H. R. Smith, and A. M. Leibhold. 1996. Interactions among gypsy moths, white-footed mice, and acorns. *Ecology* 77:2332–2342.
- Ellner, S., and P. Turchin. 1995. Chaos in a noisy world: new methods and evidence from time-series analysis. *American Naturalist* 145:343–375.
- Elton, C. 1927. *Animal ecology*. Sidgwick Jackson, London.
- Evans, H. F., and P. F. Entwistle. 1987. Viral diseases. Pages 257–322 in J. R. Fuxa and Y. Tanada, eds. *Epizootiology of insect diseases*. Wiley, New York.
- Fuxa, J. R., and A. R. Richter. 1992. Virulence and multigeneration passage of a nuclear polyhedrosis virus selected for an increased rate of vertical transmission. *Biological Control* 2:171–175.
- Gould, J. R., J. S. Elkinton, and W. E. Wallner. 1990. Density-dependent suppression of experimentally created gypsy-moth, *Lymantria dispar* (Lepidoptera: Lymantriidae) populations by natural enemies. *Journal of Animal Ecology* 59:169–184.
- Hassell, M. P., J. H. Lawton, and R. M. May. 1976. Patterns of dynamical behavior in single species populations. *Journal of Animal Ecology* 45:471–486.
- Hassell, M. P., R. M. May, S. W. Pacala, and P. L. Chesson. 1991. The persistence of host-parasitoid associations in patchy environments. I. A general criterion. *American Naturalist* 138:568–583.
- Hunter, A. F., and G. Dwyer. 1998. Insect population explosions synthesized and dissected. *Integrative Biology* 1:166–177.
- Hunter, A. F., and J. S. Elkinton. 1999. Interaction between

- phenology and density effects on mortality from natural enemies. *Journal of Animal Ecology* 68:1-9.
- . 2000. Phenology and density in the population dynamics of a forest-defoliator. *Ecology* 81:1248-1261.
- Jones, C. G., R. S. Ostfeld, M. P. Richard, E. M. Schaubert, and J. O. Wolff. 1998. Chain reactions linking acorns to gypsy moth outbreaks and Lyme disease risk. *Science* (Washington, D.C.) 279:1023-1026.
- Kermack, W. O., and A. G. McKendrick. 1927. A contribution to the mathematical theory of epidemics. *Proceedings of the Royal Society of London A* 115:700-721.
- Lance, D. R., J. S. Elkinton, and C. P. Schwalbe. 1987. Behavior of late-instar gypsy-moth larvae in high and low-density populations. *Ecological Entomology* 12: 267-273.
- Mattson, W. J., D. A. Herms, J. A. Witter, and D. C. Allen. 1991. Woody plant grazing systems: North American outbreak folivores and their host plants. U.S.D.A. Forest Service General Technical Report NE-153, 53-84.
- May, R. M. 1981. Regulation of populations with non-overlapping generations by microparasites: a purely chaotic system. *American Naturalist* 125:573-584.
- Metz, J. A. J., and O. Diekmann. 1986. *The dynamics of physiologically structured populations*. Springer, New York.
- Murray, J. D. 1993. *Mathematical biology*. Springer, Berlin.
- Murray, K. D., and J. S. Elkinton. 1989. Environmental contamination of egg masses as a major component of transgenerational transmission of gypsy-moth nuclear polyhedrosis virus (LdMNPV). *Journal of Invertebrate Pathology* 53:324-334.
- . 1990. Transmission of nuclear polyhedrosis virus to gypsy moth (Lepidoptera: Lymantriidae) eggs via contaminated substrates. *Environmental Entomology* 19:662-665.
- Murray, K. D., K. S. Shields, J. P. Burand, and J. S. Elkinton. 1991. The effect of gypsy moth metamorphosis on the development of nuclear polyhedrosis virus infection. *Journal of Invertebrate Pathology* 57:352-361.
- Myers, J. H., and B. Kuken. 1995. Changes in the fecundity of tent caterpillars: a correlated character of disease resistance or sublethal effect of disease? *Oecologia* (Berlin) 103:475-480.
- Myers J. H., G. Boettner, and J. S. Elkinton. 1999. Maternal effects in gypsy moth: only sex ratio varies with population density. *Ecology* 79:305-314.
- Onstad, D. W., J. V. Maddox, D. J. Cox, and E. A. Kornkven. 1990. Spatial and temporal dynamics of animals and the host-density threshold in epizootiology. *Journal of Invertebrate Pathology* 55:76-84.
- Ostfeld, R. S., C. G. Jones, and J. O. Wolf. 1996. Of mice and mast. *BioScience* 45:323-330.
- Podgwaite, J. D., K. S. Shields, R. T. Zerillo, and R. B. Bruen. 1979. Environmental persistence of the nucleopolyhedrosis virus of the gypsy moth virus, *Lymantria dispar*. *Environmental Entomology* 8:528-536.
- Rothman, L. D., and J. H. Myers. 1994. Nuclear polyhedrosis virus treatment effect on reproductive potential of western tent caterpillar (Lepidoptera: Lasiocampidae). *Environmental Entomology* 23:864-869.
- . 1996. Debilitating effects of viral diseases on host lepidoptera. *Journal of Invertebrate Pathology* 67:1-10.
- Turchin, P. 1990. Rarity of density dependence or population regulation with lags? *Nature* (London) 110: 1147-1153.
- Turchin, P., and A. D. Taylor. 1992. Complex dynamics in ecological time series. *Ecology* 73:289-305.
- Volkman, L. E. 1997. Nucleopolyhedrosis virus interactions with their insect host. *Advances in Virus Research* 48:313-348.
- Watanabe, H. 1987. The host population. Pages 71-112 in J. R. Fuxa and Y. Tanada, eds. *Epizootiology of insect diseases*. Wiley, New York.
- Weseloh, R. M., and T. G. Andreadis. 1986. Laboratory assessment of forest microhabitat substrates as sources of the gypsy moth nuclear polyhedrosis virus. *Journal of Invertebrate Pathology* 48:27-33.
- Williams, D. W., and A. M. Liebhold. 1995. Influence of weather on the synchrony of gypsy moth (Lepidoptera: Lymantriidae) outbreaks in New England. *Environmental Entomology* 24:987-995.
- Woods, S., and J. S. Elkinton. 1987. Bimodal patterns of mortality from nuclear polyhedrosis virus in gypsy moth (*Lymantria dispar*) populations. *Journal of Invertebrate Pathology* 50:151-157.
- Woods, S. A., J. S. Elkinton, and J. D. Podgwaite. 1989. Acquisition of nuclear polyhedrosis virus from tree stems by newly emerged gypsy moth (Lepidoptera: Lymantriidae) larvae. *Environmental Entomology* 18: 298-301.
- Woods, S., J. S. Elkinton, K. D. Murray, A. M. Liebhold, J. R. Gould, and J. D. Podgwaite. 1991. Transmission dynamics of a nuclear polyhedrosis virus and predicting mortality in gypsy moth (Lepidoptera: Lymantriidae) populations. *Journal of Economic Entomology* 84: 423-430.